Development 133, 4063-4072 (2006) doi:10.1242/dev.02581

The yolk syncytial layer regulates myocardial migration by influencing extracellular matrix assembly in zebrafish

Takuya Sakaguchi[1,2], Yutaka Kikuchi[2], Atsushi Kuroiwa[2], Hiroyuki Takeda[3,*] and Didier Y. R. Stainier[1,*]

The roles of extra-embryonic tissues in early vertebrate body patterning have been extensively studied, yet we know little about their function during later developmental events. Here, we analyze the function of the zebrafish extra-embryonic yolk syncytial layer (YSL) specific transcription factor, Mtx1, and find that it plays an essential role in myocardial migration. Downregulating the function of Mtx1 in the YSL leads to cardia bifida, a phenotype in which the myocardial cells fail to migrate to the midline. Mtx1 in the extra-embryonic YSL appears to regulate the embryonic expression of *fibronectin*, a gene previously implicated in myocardial migration. We further show dosage-sensitive genetic interactions between *mtx1* and *fibronectin*. Based on these data, we propose that the extra-embryonic YSL regulates myocardial migration, at least in part by influencing *fibronectin* expression and subsequent assembly of the extracellular matrix in embryonic tissues.

KEY WORDS: Myocardial migration, *mtx1* (*mxtx1*), Yolk syncytial layer (YSL), *fibronectin*, *natter*, Zebrafish

INTRODUCTION

Specific regions of the vertebrate extra-embryonic tissues have been shown to function as important signaling centers for early body patterning. In mammals, for example, the extra-embryonic anterior visceral endoderm (AVE) plays essential roles in forebrain induction (reviewed by Beddington and Robertson, 1999; de Souza and Niehrs, 2000). In addition, reciprocal cell-cell interactions between the extra-embryonic ectoderm and the epiblast play crucial roles in early anterior-posterior patterning and mesoderm induction during mouse embryogenesis (Brennan et al., 2001). Similarly, in zebrafish, the extra-embryonic yolk syncytial layer (YSL) is known to function as an important signaling center for mesoderm induction and early dorsoventral patterning (Mizuno et al., 1996; Chen and Kimelman, 2000) (reviewed by Sakaguchi et al., 2002). However, little is known about the roles the extra-embryonic tissues might play in later developmental events, such as organogenesis.

The heart is the first organ to form and function during vertebrate development. In all vertebrates, the heart tube develops from bilateral populations of precursor cells in the anterior lateral plate mesoderm (reviewed by McFadden and Olson, 2002). In zebrafish, these myocardial precursors migrate in between the pharyngeal endoderm and the extra-embryonic YSL toward the midline and subsequently fuse to form the functional heart tube (reviewed by Stainier, 2001; Trinh and Stainier, 2004). Large-scale forward genetic screens in zebrafish have identified mutations in eight loci that disrupt this migration process, resulting in the formation of two separate hearts, a phenotype referred to as cardia bifida (Chen et al., 1996; Stainier et al., 1996; Alexander et al., 1998). Previous analyses have demonstrated that the endodermal layer is essential for myocardial migration, as all mutants that lack pharyngeal endoderm show cardia bifida (Alexander et al., 1999; Reiter et al., 1999; Kikuchi et al., 2000). Cell transplantation analyses have further shown that wild-type endoderm can rescue the myocardial migration defects in the *casanova/sox32* mutant (David and Rosa, 2001), further supporting the idea that the pharyngeal endoderm is essential for myocardial migration. Cellular analyses have indicated that the epithelial integrity of the myocardial precursors is also important for their migration, as evidenced by the cardia bifida mutation *natter*, which affects *fibronectin 1* and appears to disrupt the polarity of the myocardial precursors (Trinh and Stainier, 2004). This finding is consistent with previous observations in mouse and chick embryos that Fibronectin, a major constituent of the extracellular matrix (ECM), is required for heart tube formation (Linask and Lash, 1988; George et al., 1993). The mechanisms that lead to cardia bifida in the *miles apart* mutant are still unclear, although the mutant exhibits dysmorphic pharyngeal endoderm (Kupperman et al., 2000). The importance of the pharyngeal endoderm in myocardial migration has been well documented; however, a role for the extra-embryonic YSL in this process has not been identified from the forward genetic analyses.

The YSL is the cortical cytoplasm region of the yolk cell, and it contains hundreds of nuclei (Trinkaus, 1992). The YSL is formed at the 500- to 1000-cell stage as marginal blastomeres collapse onto the yolk cell (Kimmel and Law, 1985). Although the YSL usually persists up to 9 days post-fertilization, it does not contribute cells or nuclei to any adult tissues (D'Amico and Cooper, 2001). Therefore, once established at the blastula stage, the YSL takes an exclusively extra-embryonic cell fate.

Several zebrafish *mix*-family genes, such as *bonnie and clyde* (*bon*), *mtx1* (*mxtx1* – Zebrafish Information Network), and *mtx2* (*mxtx2* – Zebrafish Information Network), are expressed in the YSL (Alexander et al., 1999; Hirata et al., 2000; Kikuchi et al., 2000). *bon* and *mtx2* are expressed in the marginal mesendodermal cells and the YSL, while *mtx1* is expressed exclusively in the YSL during blastula and gastrula stages (Alexander et al., 1999; Hirata et al., 2000). In higher vertebrates, *mix*-family genes such as *mixer* and *Mixl1* play important roles in endoderm and axial mesoderm development (Henry and Melton, 1998; Hart et al., 2002). In zebrafish, *bon* plays a crucial role in early endoderm differentiation

[1]Department of Biochemistry and Biophysics and Programs in Developmental Biology, Genetics and Human Genetics, Cardiovascular Research Institute, University of California, San Francisco, San Francisco, CA 94143-2711, USA. [2]Division of Biological Science, Graduate School of Science, Nagoya University, Furo-cho, Chikusa-ku, Nagoya 464-8602, Japan. [3]Department of Biological Sciences, Graduate School of Science, University of Tokyo, Hongo 7-3-1, Bunkyo-ku, Tokyo 113-0033, Japan.

*Authors for correspondence (e-mail: htakeda@biol.s.u-tokyo.ac.jp; didier_stainier@biochem.ucsf.edu)

Accepted 10 August 2006

(Kikuchi et al., 2000), and *mtx2* appears to regulate epiboly movements (Bruce et al., 2005). However, the function of *mtx1* remains unexplored.

In this study, we show that the YSL-specific gene *mtx1* is required for myocardial migration. We also show that *mtx1* regulates *natter/fibronectin 1* expression, and that *mtx1* and *natter/fibronectin 1* interact genetically. Based on these and other data, we propose that the extra-embryonic YSL regulates cardiac morphogenesis, and does so in part by regulating ECM assembly in embryonic tissues.

MATERIALS AND METHODS

Zebrafish strains

Wild-type zebrafish (*Danio rerio*) embryos were obtained from natural crosses of the Oregon AB or AB/TU heterozygote backgrounds. Homozygous or heterozygous *natter*^{tl43c} mutant embryos were obtained from incrosses and/or outcrosses of *natter* heterozygous fish. Collected embryos were maintained at 28.5°C and staged according to age [hours post-fertilization (hpf) at 28.5°C] and morphological criteria (Kimmel et al., 1995).

Injection of morpholino antisense oligonucleotides and synthesized mRNA into the YSL

Three independent antisense morpholinos (MOs) for the *mtx1* gene (Gene Tools, LLC) were injected into the YSL at the 1000-cell stage (3 hpf) as previously described (Sakaguchi et al., 2001). Eight nanograms/embryo of *mtx1* MO(A) (5′-CATCAATAGTGCTGTCTTTCCACAT-3′), 4 ng/embryo of *mtx1* MO(B) (5′-GCGTCTTCACTGGTGGAATCCTGGA-3′), 8 ng/embryo of *mtx1* MO(C) (5′-TAAACATGACAGCCCACCTGTATGC-3′), and 8 ng/embryo of 4 bp mismatch control *mtx1* MO(A) (5′-CAaC-AAaAGTGCTGTCTaTCCtCAT-3′) were injected into the YSL. Two nanograms/embryo of *laminin c1* MO (5′-TGTGTCCTTTTGCTA-TTGCGACCTC-3′) (Parsons et al., 2002) was injected into 1-cell stage embryos.

Capped sense *mtx1* mRNAs were synthesized using the mMessage mMachine in vitro transcription kit (Ambion), and purified as previously described (Sakaguchi et al., 2001). One hundred picograms/embryo of *mtx1* mRNA was injected into the YSL at the 1000-cell (3 hpf) or dome (4.3 hpf) stage.

RT-PCR and genotyping of *natter* embryos

For RT-PCR of *mtx1* cDNA, wild-type embryos and *mtx1* MO(C) injected embryos were collected at shield stage and total RNA was isolated. RT reactions were performed using the SuperScriptII RT-PCR kit (Gibco BRL) with the *mtx1* specific RT primer (5′-TCCTCAGTGGAGTGGTTATTT-AGTC-3′) according to the manufacturer's recommendations. PCR was performed using the primer pair (5′-GAGAGTCTTTCCCAAACCACAG-3′ and 5′-CATATTGTTGTAGGCTGGCAAGT-3′) to amplify *mtx1* cDNA fragments.

Genotyping by RFLP of *natter*^{tl43c} was performed by PCR as previously described (Trinh and Stainier, 2004).

In situ hybridization and immunohistochemistry

Whole-mount in situ hybridizations were performed as described (Sakaguchi et al., 2001). Immunohistochemistry was performed as described (Trinh and Stainier, 2004). We used the following antibodies: rabbit polyclonal anti-Fibronectin (Sigma) (Trinh and Stainier, 2004) at 1:200; mouse IgG_1 anti-β-catenin (Sigma) at 1:500; rabbit polyclonal anti-Laminin 1 (Sigma) at 1:200. For whole-mount anti-Laminin 1 staining, we used the ABC staining kit (Vector Laboratory) after treating with an anti-rabbit IgG biotin-conjugated antibody. Fluorescence confocal images were acquired using a Zeiss LSM5 Pascal confocal microscope.

RESULTS

Knockdown of YSL-specific transcription factor gene, *mtx1*, causes cardia bifida

As the YSL is an important signaling center during embryogenesis (reviewed by Sakaguchi et al., 2002), we screened for genes that are expressed in the YSL at the late blastula stage and examined their function by MO (Heasman, 2002) knockdown experiments. We found that an MO designed to knock down the *124H4* clone caused heart malformations and subsequently determined that the *124H4* clone is identical to the previously reported transcription factor gene *mtx1* (Hirata et al., 2000). *mtx1* is a Mix-type homeobox gene that is expressed exclusively in the YSL from the oblong stage (3.7 hpf) until 80% epiboly (8.3 hpf) (Hirata et al., 2000) (data not shown). No *mtx1* transcripts can be detected after gastrula stage, or in any embryonic tissues (Hirata et al., 2000). However, it remains theoretically possible that low levels of *mtx1* transcripts are present in embryonic tissues. In all experiments, we injected *mtx1* MOs into the YSL at the 1000-cell stage (3 hpf) to knock down *mtx1* function in this tissue. We found that *mtx1* MO(A) injected embryos displayed pericardial edema (Fig. 1B, arrowhead) and a flattened hindbrain (Fig. 1B, arrow) at 34 hpf. Injecting a 4 bp mismatch control MO into the YSL did not cause any phenotype (Fig. 1A). Interestingly, when we investigated the cause of the pericardial edema, we found that approximately 30% (14/51) of *mtx1* MO(A)-injected embryos showed cardia bifida at 34 hpf (Fig. 1D, arrowheads). Co-injection of Rhodamine Dextran with *mtx1* MO(A) allowed us to visualize the distribution of the MO and showed it to be mostly restricted to the YSL even as late as 34 hpf (Fig. 1E,F). These results indicate that the YSL regulates myocardial migration.

We further analyzed the cardia bifida phenotype of *mtx1* MO(A)-injected embryos by examining the expression of the myocardial-specific marker *cmlc2* (*myl7* – Zebrafish Information Network) (Yelon et al., 1999). We first examined myocardial migration at the 21-somite stage (19.5 hpf), a time at which the two groups of myocardial precursors initially fuse at the midline (Yelon et al., 1999). We found that 100% (14/14) of *mtx1* MO(A)-injected embryos exhibited two bilateral clusters of myocardial cells at this stage, indicating a failure in their migration to the midline (Fig. 1H). By contrast, none of the 4 bp mismatch control MO-injected embryos exhibited a myocardial migration defect (Fig. 1G). Time-lapse observations of myocardial migration with *Tg(cmlc2:GFP)* embryos (Huang et al., 2003) indicated that the myocardial precursors, which failed to fuse at the 21-somite stage, had reached the midline by 24 hpf in 4/6 of *mtx1* MO(A)-injected embryos (Fig. 1N), while in the other two cases they remained bilateral (Fig. 1O). The embryos showing delayed myocardial fusion sometimes established circulation by 34 hpf, whereas the embryos showing bilateral myocardial precursors at 24 hpf developed clear cardia bifida by 34 hpf. Consistent with these observations, we found that at 38 hpf the *cmlc2*-expressing myocardial precursors remained bilateral in approximately 30% (4/11) of *mtx1* MO(A)-injected embryos (Fig. 1Q). These results indicate that the migration of the myocardial precursors was severely compromised in *mtx1* MO(A)-injected embryos.

Specificity of *mtx1* morpholinos

To test the specificity of MO(A) for *mtx1*, we designed and injected two additional *mtx1* MOs [MO(B) and (C)] into the YSL. Both MO(B) and MO(C) caused the same phenotype as MO(A), and myocardial cells failed to fuse at the midline at the 21-somite stage in all injected embryos (16/16, 18/18, respectively; Fig. 1I,J), suggesting that the *mtx1* MOs function in a target-specific manner.

As cytoplasmic bridges connect the yolk cell to marginal blastomeres until sphere stage (4 hpf) (Cooper and D'Amico, 1996), MOs injected into the YSL before sphere stage can diffuse into embryonic tissues. As it remained formally possible that *mtx1* was expressed at very low levels in marginal blastomeres, and to assess the specificity of the MOs, we wanted to test whether

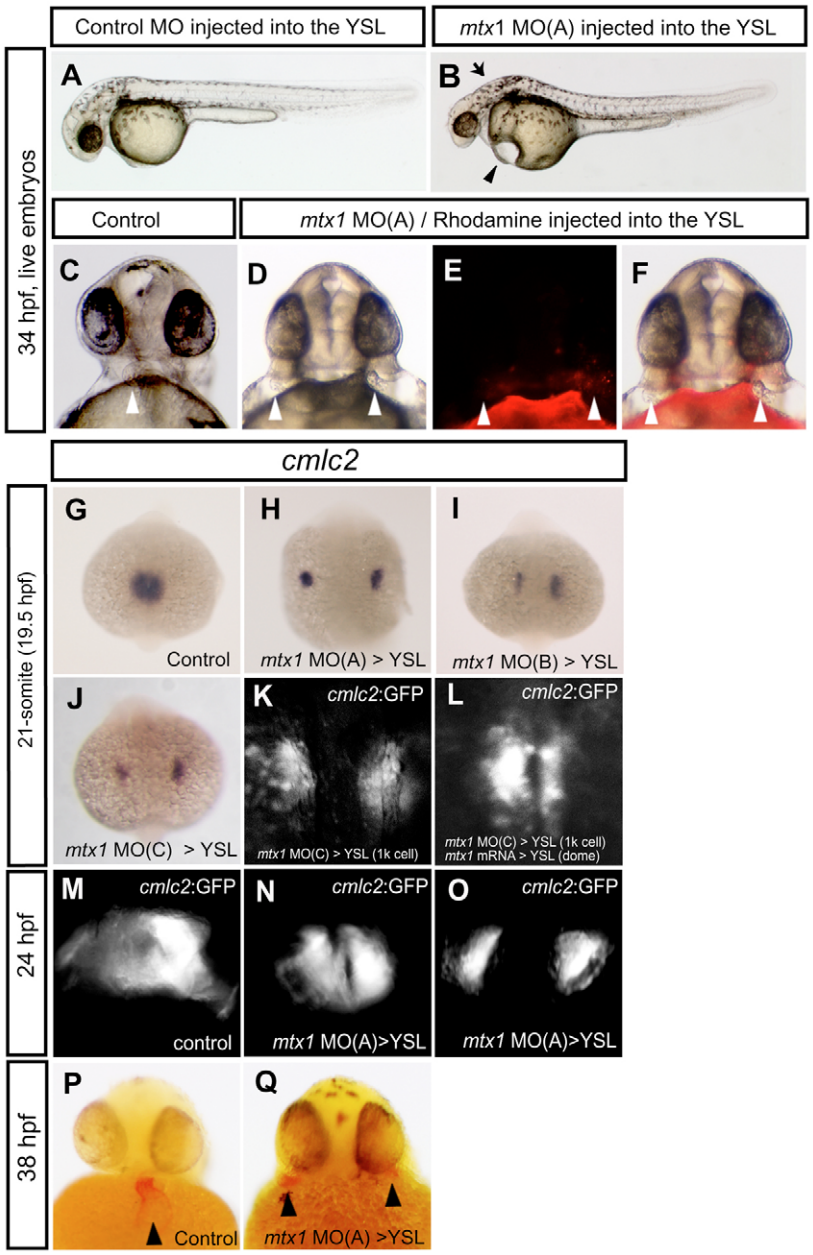

Fig. 1. The YSL regulates myocardial migration. Embryos injected with a 4 bp mismatch *mtx1* control MO (A,C,G), *mtx1* MO(A) (B,D-F,H,N-O,Q), *mtx1* MO(B) (I) or *mtx1* MO(C) (J,K), into the YSL at the 1000-cell stage (3 hpf), embryos injected with *mtx1* MO(C) into the YSL at the 1000-cell stage and *mtx1* mRNA into the YSL at dome stage (L), and uninjected control embryos (M,P). (**A-F**) Live embryos at 34 hpf. (A,B) Lateral views, anterior to the left. *mtx1* MO(A)-injected embryos exhibit cardiac edema (arrowhead) and a flattened hindbrain ventricle (arrow) (B). (C-F) Frontal views reveal the cardiac phenotype of control and *mtx1* MO(A)-injected embryos. Approximately 30% of *mtx1* MO(A)-injected embryos showed a clear cardia bifida phenotype at 34 hpf (D). Rhodamine Dextran was co-injected with *mtx1* MO(A) to visualize the distribution of the injected solution, and this method revealed that it was mostly restricted to the YSL. Bright field (D) and fluorescent views (E) are merged in F. White arrowheads point to the cardiac tissues. Expression of the myocardial-specific markers, *cmlc2* (**G-J**,**P**,**Q**) and *Tg(cmlc2:GFP)* (**K-O**), in embryos injected with *mtx1* MOs into the YSL. (G-O) Dorsal views, anterior to the top. (P,Q) Frontal views, arrowheads point to the myocardial clusters. At the 21-somite stage (19.5 hpf), myocardial cells have fused at the midline and form a shallow cardiac cone in control MO-injected embryos (G), whereas they remained bilateral in *mtx1* MO-injected embryos (H-K). (H-K) Three independent *mtx1* MOs, MO(A) (H), MO(B) (I), and MO(C) (J,K), caused the same phenotype in a fully penetrant manner when examined at the 21-somite stage (19.5 hpf). (L) *mtx1* mRNA injection into the YSL at dome stage rescued the myocardial migration defect of *mtx1* MO(C)-injected embryos (21-somite stage, 19.5 hpf, shown). At 24 hpf, myocardial cells have fused at the midline and begun to form a tube that extends toward the left anterior part of control uninjected embryos (M), whereas myocardial cells have just fused (N) or not yet fused (O) in *mtx1* MO(A)-injected embryos. At 38 hpf, myocardial cells form a single tubular functioning heart in uninjected control embryos (P), but these cells formed two clearly distinct structures in approximately 30% of *mtx1* MO(A)-injected embryos (Q).

restoring *mtx1* mRNA specifically in the YSL would rescue the myocardial migration phenotype of *mtx1* MO-injected embryos. We injected *mtx1* MO(C) into the YSL at the 1000-cell stage (3 hpf) and subsequently injected some of these embryos with *mtx1* mRNA into the YSL at dome stage (4.3 hpf). While all (n=8) of the embryos injected with *mtx1* MO(C) showed delayed myocardial migration at the 21-somite stage (Fig. 1K), 50% (3/6) of the embryos subsequently injected with *mtx1* mRNA into the YSL exhibited wild-type-like myocardial migration (Fig. 1L). These data indicate that *mtx1* functions in the YSL to regulate myocardial migration.

Of the three *mtx1* MOs tested, two of them [MO(A) and MO(B)] were designed to block translation initiation of *mtx1* mRNA, and the other [MO(C)] was designed against the splice donor site of the second exon in order to interfere with splicing (Fig. 2A). RT-PCR analysis revealed that MO(C) blocked the endogenous splice site of *mtx1* and, as a result, an additional 20 bp was inserted into the *mtx1* mRNA, leading to a frame shift and premature translation stop (Fig. 2A,B). This result further illustrates the efficiency and specificity of *mtx1* MOs.

Endoderm development in *mtx1* knockdown embryos

As endoderm formation is known to be essential for myocardial migration in zebrafish (reviewed by Stainier, 2001), we first asked whether endoderm development in *mtx1* MO-injected embryos was affected. Expression of early endoderm markers, such as *sox17* (Alexander and Stainier, 1999) and *casanova/sox32* (Dickmeis et al., 2001; Kikuchi et al., 2001; Sakaguchi et al., 2001), appeared unaffected in *mtx1* MO(A)-injected embryos (Fig. 3A-D), indicating that the loss of *mtx1* function does not affect early endoderm formation. Later in development, myocardial cells migrate underneath a sheet of pharyngeal endoderm toward the midline (Trinh and Stainier, 2004). Therefore, we examined pharyngeal

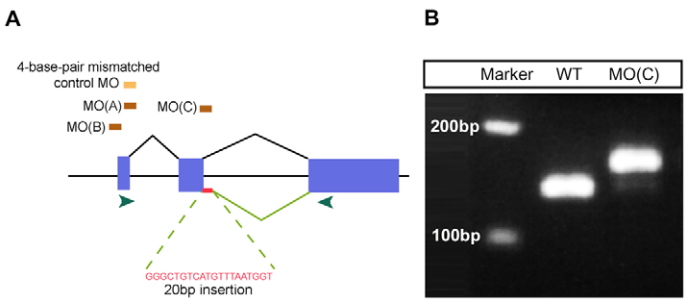

Fig. 2. Specificity of *mtx1* MOs. (**A**) Schematic diagram of *mtx1* genomic structure and position of *mtx1* MOs. *mtx1* has three exons (blue boxes) and two introns. Two independent ATG MOs, MO(A) and MO(B), and a splice donor MO, MO(C), caused essentially the same phenotype when injected into the YSL at the 1000-cell stage. The splice donor MO, *mtx1* MO(C), leads to a 20 bp insertion in *mtx1* mRNA, which leads to a frame shift and premature termination. Green arrowheads indicate the position of the primers used for the RT-PCR analysis shown in B. (**B**) RT-PCR analysis shows that an additional 20 bp are integrated into *mtx1* mRNA in *mtx1* MO(C)-injected embryos.

endoderm development in *mtx1* MO(A)-injected embryos and it appeared unaffected, as assessed by examining the pharyngeal endoderm-specific GFP expression in *Tg(her5:GFP)*^{ne206} embryos (Tallafuss and Bally-Cuif, 2003) at the 18-somite stage (Fig. 3E,F). Despite the absence of obvious pharyngeal endoderm defects, these embryos exhibited myocardial migration defects at the 21-somite stage (data not shown), indicating that *mtx1* had been knocked down in these embryos. We also examined *Tg(her5:GFP)*^{ne2067}*; Tg(cmlc2:GFP)* embryos in cross-sections and did not detect any obvious defects in *her5:GFP* expression in *mtx1* MO-injected

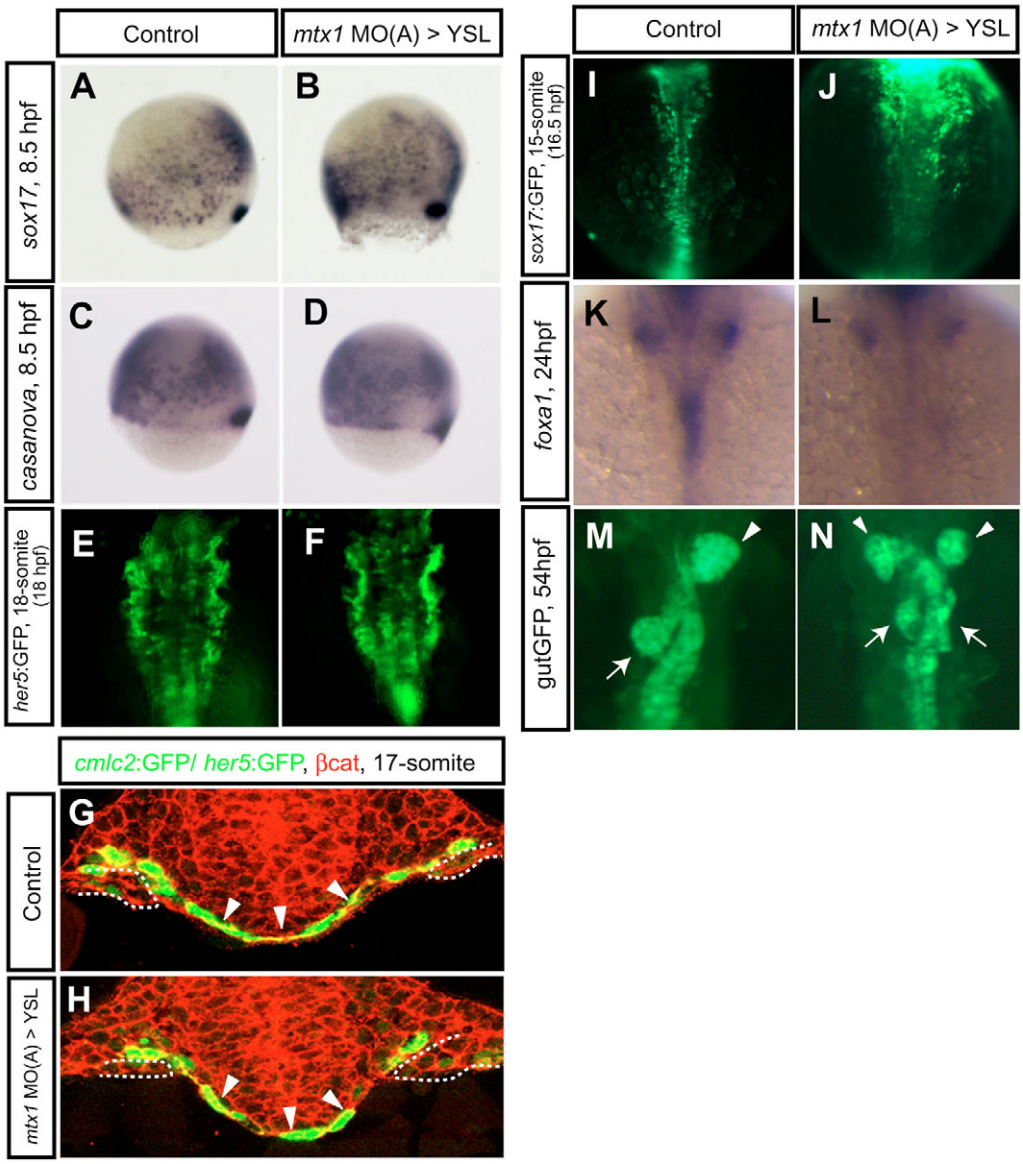

Fig. 3. Endoderm development in *mtx1* MO-injected embryos. Endoderm differentiation and morphology in wild-type embryos (A,C,E,G,I,K,M) and embryos injected with *mtx1* MO(A) into the YSL (B,D,F,H,J,L,N). Expression of early endoderm markers, *sox17* (**A**,**B**) and *casanova/sox32* (**C**,**D**), at 80% epiboly (8.5 hpf) did not appear to be affected in *mtx1* MO(A)-injected embryos. (**E**,**F**) Anterior views of *her5*:GFP transgenic embryos at the 18-somite stage show unaffected pharyngeal endoderm development. (**G**,**H**) The pharyngeal endoderm was also examined in transverse confocal images (dorsal at the top) of *Tg(cmlc2:GFP); Tg(her5:GFP)*^{ne2067} embryos counterstained for β-catenin (red). Arrowheads point to the pharyngeal endoderm and dashed lines outline the myocardial cells in the lateral plate mesoderm. (**I**,**J**) Dorsal views of the mid-trunk region of *sox17*:GFP transgenic embryos at the 15-somite stage. Anterior to the top. *sox17*:GFP-positive endodermal cells in the future foregut region are coalescing toward the midline in control embryos (I), whereas they appeared to be delayed in their migration in *mtx1* MO(A)-injected embryos (J). (**K**,**L**) Dorsal views of *foxa1* expression in the digestive organ-forming region at 24 hpf. By 24 hpf, endodermal cells have already coalesced at the midline and formed a rod in wild-type embryos (K), whereas they remained as a sheet in *mtx1* MO(A)-injected embryos (L). (**M**,**N**) Ventral views of *gutGFP* expression at 54 hpf. Approximately 30% of *mtx1* MO-injected embryos showed duplicated hepatic (white arrowheads) and pancreatic (white arrows) buds at this stage (N), further illustrating the endoderm morphogenesis defects.

embryos at the level of the cardiac mesoderm at the 17-somite stage (17.5 hpf) (Fig. 3G,H). These data suggest that the YSL regulates myocardial migration independently of pharyngeal endoderm formation.

Although the pharyngeal endoderm did not appear to be disrupted in *mtx1* MO-injected embryos, we found that more posterior endoderm, which gives rise to the liver and pancreas, appeared to be affected. The posterior endoderm forms a wide sheet-like structure at early segmentation stages and subsequently condenses into a rod-like structure at the midline by 24 hpf (Field et al., 2003; Ober et al., 2003). We were able to visualize these condensing foregut endodermal cells at the 15-somite stage with a *sox17*-promoter-GFP transgenic line, *Tg(sox17:GFP)*^{s870} (Y.K. and W. Chung, unpublished) (Fig. 3I). In *mtx1* MO(A)-injected embryos at the 15-somite stage, foregut endodermal cell migration appeared to be delayed, as evidenced by its sheet-like appearance (Fig. 3J). By 24 hpf, foregut endodermal cells, marked by *foxa1* expression, have already formed a rod in control embryos (Fig. 3K), whereas this cell migration was delayed in *mtx1* MO(A)-injected embryos (12/15; Fig. 3L). Due to this cell migration delay, approximately 30% (6/18) of *mtx1* MO(A)-injected embryos developed duplicated hepatic and anterior pancreatic buds, as assessed by *Tg(gutGFP)*^{s854} (Field et al., 2003; Ober et al., 2003) expression at 54 hpf (Fig. 3M,N). As endodermal cells migrate on the YSL to coalesce at the midline, the YSL is probably also regulating this process.

natter/fibronectin 1 is regulated by mtx1

To investigate the mechanisms by which the YSL regulates myocardial migration, we next focused on the *natter/fibronectin 1* gene, which, like *mtx1*, is necessary for myocardial migration but appears to act independently from the endoderm (Trinh and Stainier, 2004). In addition, *mtx1* MO-injected embryos exhibited similar phenotypes to those of *natter/fibronectin 1* mutants, such as a flattened hindbrain and a partially penetrant cardia bifida (Fig. 1B, Fig. 5C) (Trinh and Stainier, 2004). We analyzed *natter/fibronectin 1* expression in *mtx1* MO(A)-injected embryos at several stages and detected a clear downregulation at the 14-somite stage (16 hpf) in the anterior lateral plate mesoderm, when the myocardial precursors start to migrate to the midline (Fig. 4A,B). This downregulation of *natter/fibronectin 1* expression was also detected at the 21-somite stage (19.5 hpf), when the myocardial precursors first fuse at the midline (Fig. 4C,D). At the 21-somite stage, *natter/fibronectin 1* is expressed in the laterally located myocardial cells and medially located endocardial cells (Trinh and Stainier, 2004). We observed a downregulation of *natter/fibronectin 1* expression in both cell populations in *mtx1* MO(A)-injected embryos (Fig. 4D). We also examined Fibronectin protein deposition in *mtx1* MO(A)-injected embryos. In wild-type embryos at the 18-somite stage, Fibronectin is deposited on the basal side of the myocardial precursors as well as on the basal side of the pharyngeal endoderm (Fig. 4I) (Trinh and Stainier, 2004). In *mtx1* MO(A)-injected embryos, Fibronectin deposition was greatly reduced around both the myocardial precursors and the pharyngeal endoderm (Fig. 4J).

As loss of *mtx1* function downregulated *natter/fibronectin 1* gene expression, we next asked whether *mtx1* overexpression could alter *natter/fibronectin 1* expression. Initially, we injected 100 pg *mtx1* mRNA into 1-cell-stage embryos; however, these injected embryos showed severe gastrulation and epiboly defects. We then injected the same amount of *mtx1* mRNA into the YSL at the 1000-cell stage to overexpress *mtx1* preferentially in this tissue. We found that all these injected embryos appeared morphologically unaffected at 34 hpf (data not shown). However, interestingly, we found that

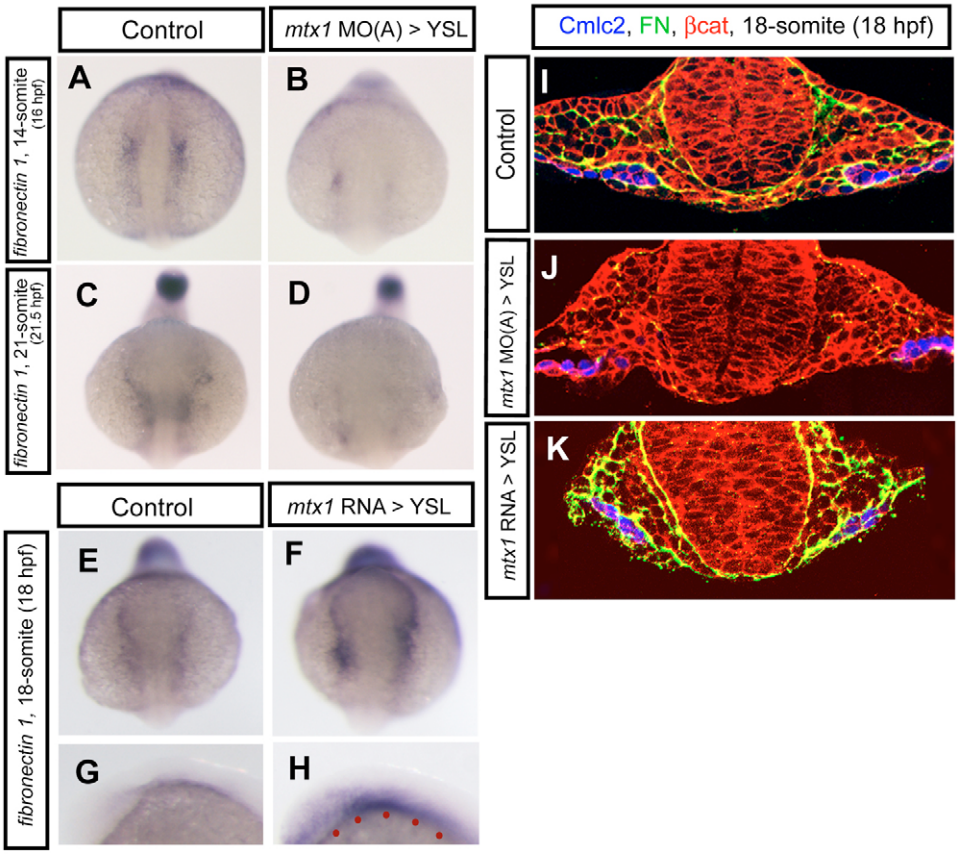

Fig. 4. *fibronectin 1* expression is regulated by *mtx1*. *fibronectin 1* gene expression and Fibronectin protein localization around the migrating myocardial cells were examined in embryos injected into the YSL with *mtx1* MO(A) or *mtx1* mRNA. (A-F) Anterior views, (G,H) Lateral views in the head region. (**A-H**) *fibronectin 1* expression at the 14- (A,B; 16 hpf), 18- (E-H; 18 hpf), and 21-somite stages (C,D; 21.5 hpf). (A-D) *fibronectin 1* expression appeared to be reduced in *mtx1* MO(A)-injected embryos. (E-H) Conversely, *fibronectin 1* expression appeared to be increased in *mtx1* mRNA-injected embryos. (F,H) *fibronectin 1* expression was upregulated mostly in embryonic tissues, even though *mtx1* mRNA was injected into the YSL (red dots in H), indicating that *mtx1* regulates *fibronectin 1* expression in a non-cell-autonomous manner. (**I-K**) Transverse sections of *cmlc2*:GFP (false colored blue) transgenic embryos immunostained for β-catenin (red) and Fibronectin (green). Fibronectin deposition appeared to be decreased in *mtx1* MO-injected embryos (J), whereas it appeared to be increased in *mtx1* mRNA-injected embryos (K) specifically in embryonic tissues.

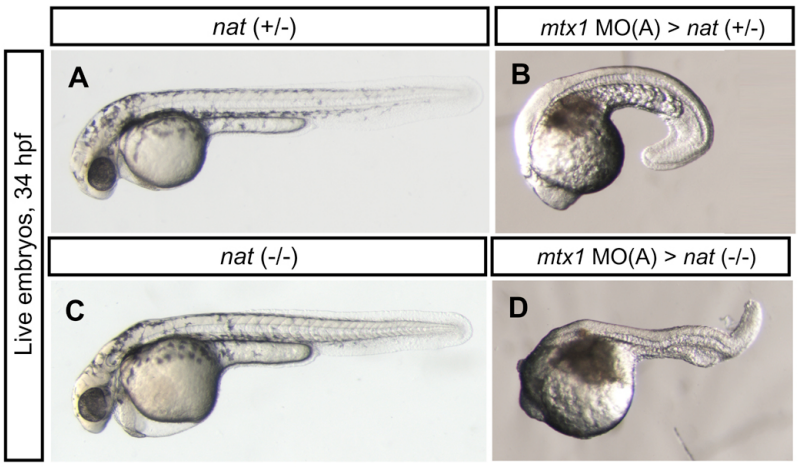

Fig. 5. Genetic interaction between *natter/fibronectin 1* and *mtx1*. (**A-D**) Lateral views of bright field images at 34 hpf, anterior to the left. (A) *natter* heterozygote, (C) *natter* homozygous mutant, (B) *natter* heterozygote injected with *mtx1* MO(A) into the YSL and (D) *natter* homozygous mutant injected with *mtx1* MO(A) into the YSL. The partial or complete reduction of *fibronectin 1* in *mtx1* MO-injected embryos uncovered novel phenotypes.

natter/fibronectin 1 expression in the anterior lateral plate mesoderm of these embryos appeared to be upregulated at the 18-somite stage (Fig. 4E-H). Fibronectin immunoreactivity was also clearly increased in embryonic tissues (Fig. 4K). These data suggest that the extra-embryonic YSL is regulating embryonic *natter/fibronectin 1* expression in adjacent embryonic tissues.

Genetic interaction between *mtx1* and *natter/fibronectin 1*

To further investigate the relationship between *mtx1* and *fibronectin 1*, we tested for genetic interaction. For this purpose, we injected *mtx1* MO(A) into embryos obtained from crossing heterozygote *natter* parents, and surprisingly found that approximately three-quarters of these injected embryos exhibited a severely enhanced phenotype (Fig. 5B,D), while another quarter showed exactly the same phenotype as *mtx1* MO-injected embryos (Fig. 1B). Genotyping the affected and unaffected embryos revealed that injecting *mtx1* MO(A) into heterozygous *natter* embryos enhanced the *mtx1* MO injection phenotype (Fig. 5B): at 34 hpf, the head of these embryos appeared to be collapsed onto the yolk ball, the somite boundaries were not easily distinguishable, and pigmentation appeared to be delayed (Fig. 5B). These embryos survived at least until 50 hpf, suggesting that they were not dying simply from non-specific effects of the MO. These data indicate that *mtx1* and *natter/fibronectin 1* interact in a dosage-dependent manner, suggesting that they work in the same or interacting pathways.

Homozygous *natter* mutant embryos injected with *mtx1* MO(A) frequently failed to complete epiboly and died after yolk rupture during gastrulation (data not shown). The embryos that survived appeared similar to *mtx1* MO(A)-injected heterozygous *natter* embryos at 34 hpf (Fig. 5D).

Morphogenesis of *mtx1* MO-injected heterozygous *natter* embryos

As *mtx1* MO-injected heterozygous *natter* embryos showed severe morphogenetic defects, we carried out a time-course analysis to determine how these defects developed during embryogenesis (Fig. 6). *mtx1* MO-injected heterozygous *natter* embryos appeared normal at the tailbud stage (Fig. 6A,F; 10 hpf). However, 2 hours later, at the 6-somite stage, the YSL at the hindbrain level started to

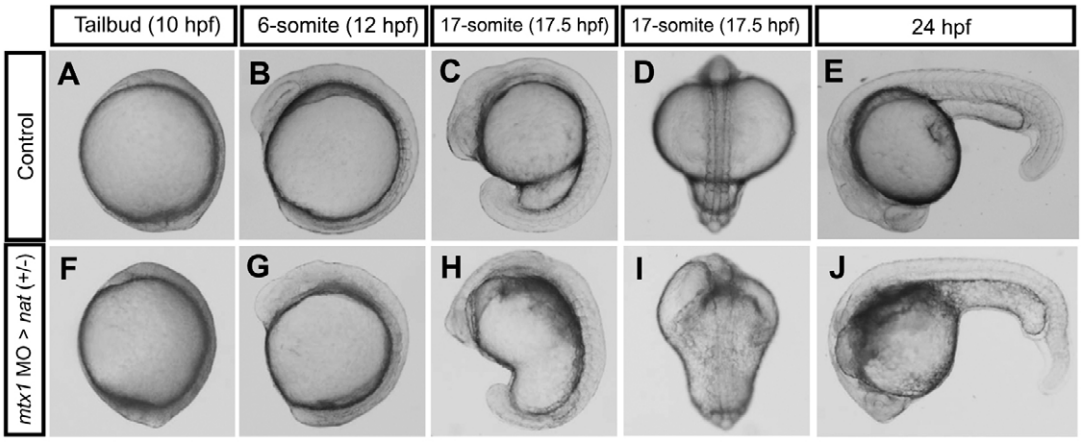

Fig. 6. Morphogenesis of *mtx1* MO-injected heterozygous *natter* embryos. (**A-E**) Wild-type embryo; same embryo is shown at all stages. (**F-J**) heterozygous *natter* embryo injected with *mtx1* MO(A) into the YSL at the 1000-cell stage; same embryo is shown at all stages. Lateral views, animal pole up and dorsal to the right (A-C,F-H); dorsal views, animal pole up (D,I), lateral views, anterior to the left and dorsal up (E,J). *mtx1* MO-injected heterozygous *natter* embryo showed no apparent defect at the tailbud stage (A,F). A phenotype first appeared at the 6-somite stage at the hindbrain level as the YSL got darker (G). At the 17-somite stage, the head ventricle was almost collapsed onto the YSL (I). At 24 hpf, somite boundaries are clearly visible in wild-type embryos (E), whereas they were harder to visualize in *mtx1* MO-injected heterozygous *natter* embryos (J), especially in the anterior part.

darken (Fig. 6B,G; 12 hpf). By the 17-somite stage (17.5 hpf), the head structure appeared to be collapsing onto the YSL in *mtx1* MO-injected heterozygous *natter* embryos (Fig. 6C-D,H-I). At 24 hpf, somite boundaries became hard to distinguish, especially in the anterior part (Fig. 6E,J). This result is consistent with previous observations that *natter/fibronectin 1* and *fibronectin 3* are required for somite formation (Julich et al., 2005; Koshida et al., 2005). By 34 hpf, the hindbrain was completely collapsed onto the yolk ball and most somite boundaries appeared to be missing (Fig. 5B). These data show that major defects appeared at late segmentation stages in *mtx1* MO-injected heterozygous *natter* embryos.

The YSL influences embryonic extracellular matrix assembly

To characterize in more detail *mtx1* MO-injected heterozygous *natter* embryos, we analyzed the expression of regional specification markers for the hindbrain, somites and heart. Although the morphology of *mtx1* MO-injected heterozygous *natter* embryos appeared to be severely disrupted (Fig. 6), the expression of the midbrain-hindbrain boundary marker *paxb* (*pax2a* – Zebrafish Information Network) (Fig. 7A,B) (Krauss et al., 1991), the rhombomeres 3 and 5 marker *krox20* (*egr2b* – Zebrafish Information Network) (Fig. 7A,B) (Oxtoby et al., 1993), and the adaxial cell and segmented somite marker *myod* (Fig. 7C,D) (Weinberg et al., 1996) appeared in a properly segmented manner, indicating that these embryos were being patterned properly. Also, although myocardial cells failed to migrate in these embryos, they continued to express the myocardial marker *cmlc2* (Fig. 7E,F).

To further understand why *mtx1* MO-injected heterozygous *natter* embryos could not maintain their morphology, we examined ECM assembly by analyzing Laminin 1 immunoreactivity (Parsons et al., 2002; Pollard et al., 2006). We found that *mtx1* MO-injected heterozygous *natter* embryos exhibited greatly reduced Laminin 1 immunoreactivity in the hindbrain at 24 hpf, while it appeared unchanged in their trunk and tail (Fig. 7H,J). Confocal images of cross-sections at the level of the cardiac mesoderm further illustrated the fact that Laminin 1 immunoreactivity was reduced in *mtx1* MO-injected heterozygous *natter* embryos (Fig. 7L). As *mtx1* MO injections into wild-type embryos did not significantly reduce Laminin 1 immunoreactivity (data not shown), these data suggest that losing one copy of *natter/fibronectin 1* in the absence of *mtx1* function leads to a further disruption of ECM assembly.

To further analyze the role of the YSL in ECM assembly, we injected *mtx1* MO(A) into the YSL of embryos previously injected with *laminin c1* (*lamc1*) MO at the 1-cell stage. *lamc1* encodes Laminin γ1 and is essential for notochord differentiation and Laminin 1 immunoreactivity (reviewed by Stemple, 2005; Parsons et al., 2002; Pollard et al., 2006). Embryos injected with *lamc1* MO

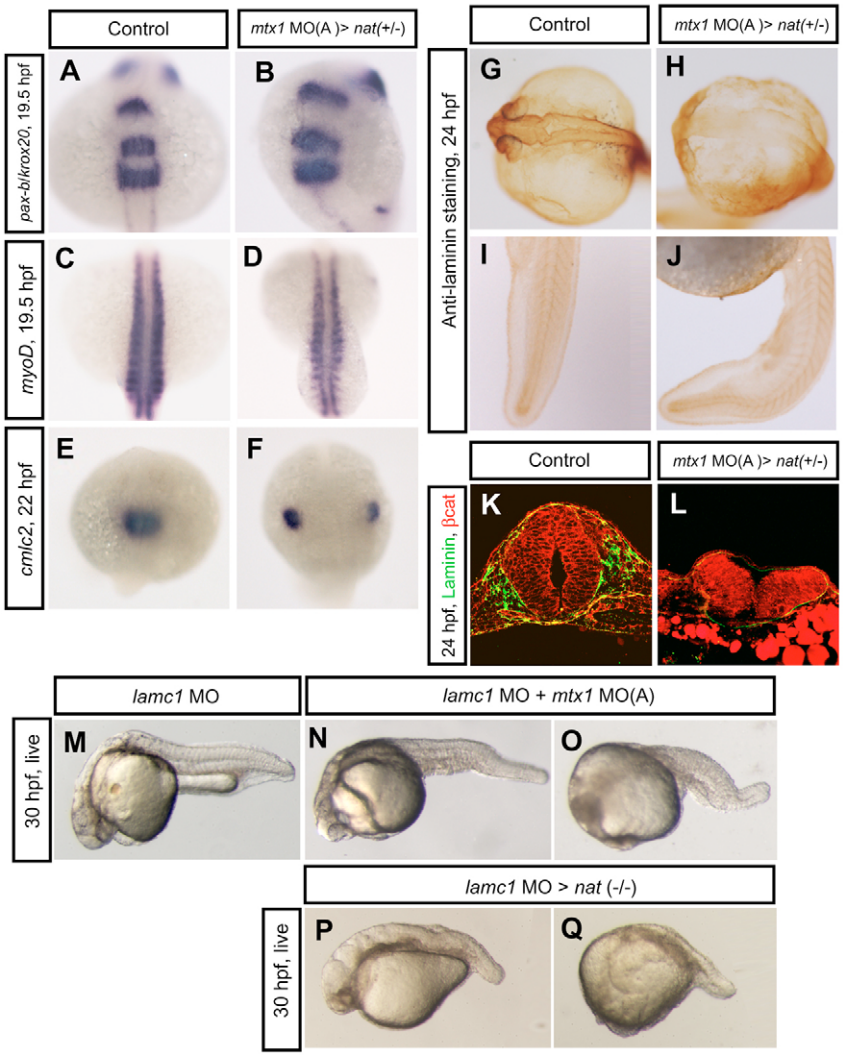

Fig. 7. Regional specification and ECM formation in *mtx1* MO-injected heterozygous *natter* embryos. (**A**,**B**) Dorsal views of hindbrain, (**C**,**D**) somite and (**E**,**F**) heart regions. *pax-b* and *krox20* expression in the midbrain-hindbrain boundary and rhombomeres 3 and 5 at 19.5 hpf (A,B), and *myod* expression in the segmented somites and adaxial cells at 19.5 hpf (C,D), appeared unaffected in *mtx1* MO-injected heterozygous *natter* embryos. (E,F) *cmlc2* expression in the myocardial cells at 22 hpf reveals that *mtx1* MO-injected heterozygous *natter* embryos displayed cardia bifida. (**G-L**) Laminin immunostaining at 24 hpf. Laminin deposition appeared to be greatly reduced in the hindbrain region of *mtx1* MO-injected *natter* heterozygous embryos (H), but not in the trunk and tail (J). (K,L) Transverse sections of embryos (anterior region) immunostained for β-catenin (red) and Laminin (green). Laminin deposition was greatly downregulated and the head structure collapsed in *mtx1* MO-injected heterozygous *natter* embryos (L). (**M-Q**) Lateral views of bright field images at 30 hpf, anterior to the left. Embryos injected with *laminin c1* MO at the 1-cell stage exhibited shortened body axis and defects in notochord differentiation (M). Embryos injected with *lamimin c1* MO at the 1-cell stage and *mtx1* MO(A) into the YSL at the 1000-cell stage showed enhanced phenotypes in the hindbrain region (N) or entire head region (O). Homozygous *natter* mutant embryos injected with *laminin c1* MO (P,Q).

at the 1-cell stage exhibited a shortened body axis and defects in notochord differentiation at 30 hpf (Fig. 7M) (Parsons et al., 2002). When we injected *mtx1* MO(A) into the YSL of embryos previously injected with *lamc1* MO, approximately 50% of embryos (47/90) appeared to die after yolk rupture during segmentation stages. Surviving embryos appeared to exhibit an enhanced phenotype, in which body structures were collapsing in the hindbrain region (22/90) (Fig. 7N) or in the entire head region (17/90) (Fig. 7O) at 30 hpf. These phenotypes were not seen in *lamc1* MO-injected embryos or *mtx1* MO(A)-injected embryos. These results further support the idea that the YSL influences embryonic ECM assembly.

We also injected *lamc1* MO into embryos obtained from crossing heterozygote *natter* parents. Approximately a quarter of these injected embryos (14/44) exhibited a severely enhanced phenotype (Fig. 7P,Q), while another three-quarters showed exactly the same phenotype as *lamc1* MO-injected embryos (Fig. 7M). Genotyping the affected and unaffected embryos showed that injecting *lamc1* MO into homozygous but not heterozygous *natter* embryos enhanced their phenotype (Fig. 7P,Q). These results indicate that embryos lacking multiple components of the ECM can exhibit enhanced phenotypes.

DISCUSSION

Our data indicate that the YSL-specific transcription factor, Mtx1, regulates *natter/fibronectin 1* gene expression in the lateral plate mesoderm. As *natter/fibronectin 1* is required for myocardial migration (Trinh and Stainier, 2004), loss of Mtx1 function also leads to cardia bifida. Interestingly, we also found a genetic interaction between *mtx1* and *natter/fibronectin 1*. Taken together, these data indicate that the extra-embryonic YSL regulates cardiac morphogenesis, at least in part by the *mtx1-natter/fibronectin 1* pathway.

Specificity of *mtx1* MOs

In this study, we injected *mtx1* MOs into the YSL at the 1000-cell stage (3 hpf) to knock down *mtx1* function in the YSL. All three *mtx1* MOs caused the same phenotype, as assessed by the expression of the myocardial marker *cmlc2* at the 21-somite stage (Fig. 1H-J). These data strongly suggest that *mtx1* MOs function in a target-specific manner. Injection of the *mtx1* MO(C) into 1-cell-stage embryos caused cardia bifida, although at low frequency (data not shown). As the YSL contains hundreds of nuclei, we suspect that knocking down genes in the YSL requires a higher concentration of MOs, one achieved by YSL injections.

We propose that our *mtx1* MO injections are specifically knocking down *mtx1* function in the YSL for the following reasons: first, *mtx1* appears to be exclusively expressed in the YSL (Hirata et al., 2000), and we injected *mtx1* MOs into this tissue. Second, the same concentration of a 4 bp mismatch *mtx1* MO(A) did not cause any obvious phenotypes when injected into the YSL (Fig. 1A,G). Third, the splice donor MO, *mtx1* MO(C), leads to a frame shift and premature translational termination of *mtx1* (Fig. 2). Finally, restoring *mtx1* mRNA in the YSL rescued the myocardial migration defect (Fig. 1L).

Roles of the extra-embryonic YSL in myocardial migration

In zebrafish, myocardial precursors migrate in between the endodermal layer and the extra-embryonic YSL (Fig. 8A) (Trinh and Stainier, 2004) (reviewed by Stainier, 2001). Previous studies have demonstrated that the endodermal layer is essential for myocardial migration (reviewed by Stainier, 2001). This study clearly illustrates for the first time that the extra-embryonic YSL also plays important roles in myocardial migration.

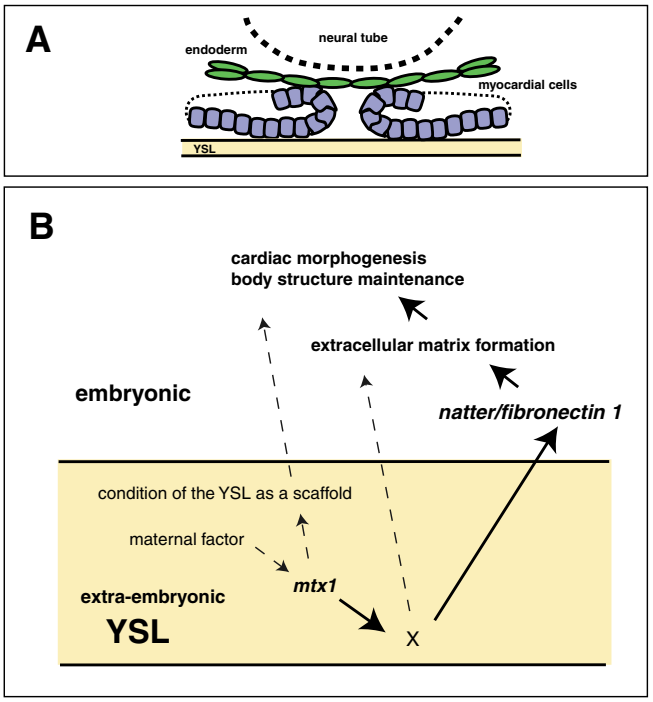

Fig. 8. Model of YSL function during early cardiac morphogenesis. (**A**) Diagram represents transverse section of myocardial precursors (blue) within the lateral plate mesoderm (dotted line) during myocardial migration. Myocardial cells migrate between the endodermal layer (green) and the extra-embryonic YSL (yellow). (**B**) Model of *mtx1* function in the YSL in myocardial migration. *mtx1* is expressed exclusively in the extra-embryonic YSL. *mtx1* is probably responsible for regulating the differentiation of the YSL as a tissue on which many cell types, including myocardial and endodermal cells, migrate. *mtx1* also appears to regulate an unidentified factor X in the YSL, which works in a non-cell-autonomous manner to regulate embryonic *natter/fibronectin 1* expression. This pathway is responsible, at least in part, for ECM formation, which itself is essential for early cardiac morphogenesis and body structure maintenance. Other ECM components, such as Laminin, are also probably regulated by *mtx1*. Solid lines indicate connections supported by the data presented in this study, while dashed lines indicate potential connections suggested by the data.

As *mtx1* is a strictly zygotically expressed gene, a maternal factor probably controls *mtx1* gene expression (Fig. 8B). *mtx2*, which is expressed in the YSL and marginal cells (Hirata et al., 2000), appears to be regulated by the maternal factor Eomesodermin (Bruce et al., 2005). However, Eomesodermin does not appear to regulate *mtx1* gene expression (Bruce et al., 2005), indicating that another maternal factor is involved. Interestingly, the phenotype of *mtx1* MO-injected heterozygous *natter* embryos appears similar to that of the maternal mutant *pollywog* (Fig. 5B) (Wagner et al., 2004), suggesting that Pollywog is an upstream regulator of *mtx1*.

Once *mtx1* expression is established in the YSL, it appears to regulate embryonic *natter/fibronectin1* gene expression in a non-cell-autonomous manner (Fig. 4). It is striking that loss of *mtx1* function leads to downregulation of *natter/fibronectin 1* expression

and that, by contrast, gain of *mtx1* function leads to upregulation of *natter/fibronectin 1* expression in the anterior lateral plate mesoderm. However, the *natter/fibronectin 1* gene cannot be a direct target of Mtx1, as their expression patterns do not appear to overlap. No *fibronectin 1* transcripts can be detected at shield stage (Trinh and Stainier, 2004), when *mtx1* is expressed most strongly (Hirata et al., 2000). Zygotic *fibronectin 1* expression appears to initiate at 60% epiboly (6.5 hpf) in the marginal blastomeres but not in the YSL (Trinh and Stainier, 2004), while *mtx1* appears to be expressed only in the YSL until 80% epiboly (8.3 hpf) (Hirata et al., 2000). Therefore, the regulation of *natter/fibronectin 1* by Mtx1 is probably indirect. Our data suggest that factors unidentified to date are regulated by Mtx1 in the YSL and work non-cell-autonomously to regulate *natter/fibronectin 1* expression in the embryonic lateral plate mesoderm at mid-segmentation stages (Fig. 7). Further investigation will be required to identify the molecules that function downstream of *mtx1* and upstream of *natter/fibronectin 1*. The steroidogenic enzyme Cyp11a1 (Hsu et al., 2006) and Rac-GAP Chimerin 1 (Leskow et al., 2006) have been reported to function in the YSL to regulate epiboly cell movement. It will be interesting to investigate the role of these proteins in *natter/fibronectin 1* gene expression and myocardial migration.

mtx1 might be working together with *casanova/sox32*, which is expressed in the endoderm and YSL and is responsible for endoderm formation (Dickmeis et al., 2001; Kikuchi et al., 2001; Sakaguchi et al., 2001). Although *casanova* MO injections into the YSL did not cause any obvious morphological phenotype (Sakaguchi et al., 2001), co-injection of *mtx1* and *casanova* MOs into the YSL dramatically increased the penetrance of cardia bifida at 34 hpf (data not shown). More detailed analysis will be required to further investigate this potential interaction between *casanova* and *mtx1*.

The idea that *mtx1* regulates *natter/fibronectin 1* gene expression is also supported by the fact that *mtx1* and *natter/fibronectin 1* show dosage-sensitive genetic interactions (Fig. 5). The phenotype of *mtx1* MO-injected heterozygous *natter* embryos (Fig. 5B) is much more severe than that of *mtx1* MO-injected wild-type embryos (Fig. 1B) or uninjected homozygous *natter* mutant embryos (Fig. 5C), implying that there is another pathway downstream of *mtx1*, working in parallel to the *mtx1-natter/fibronectin 1* pathway (Fig. 8). Based on our observation that Laminin 1 immunoreactivity is greatly downregulated in *mtx1* MO-injected heterozygous *natter* embryos (Fig. 7G-L), while it is not significantly affected in *mtx1* MO-injected wild-type embryos, ECM components other than Fibronectin also appear to be regulated by *mtx1* (Fig. 8). This idea is further supported by the observation that embryos injected with both *lamc1* and *mtx1* MOs showed a much more severe phenotype than that of *lamc1* MO-injected embryos (Fig. 7M), *mtx1* MO-injected embryos (Fig. 1B), or an addition of these two phenotypes. These data suggest that lacking multiple components of the ECM can lead to synergistic defects. We therefore propose that the extra-embryonic YSL regulates heart organogenesis and body structure maintenance at least in part by controlling ECM assembly (Fig. 8).

The YSL as a scaffold on which many cell types migrate

Although *mtx1* MO-injected embryos developed normal pharyngeal endoderm, they exhibited foregut endoderm migration defects (Fig. 3). This foregut endoderm phenotype is not seen in *natter* mutants (Trinh and Stainier, 2004), indicating that foregut endoderm migration is not regulated by the *mtx1-natter/fibronectin 1* pathway. Vegfc has been shown previously to regulate foregut endoderm migration (Ober et al., 2004), and it will be interesting to investigate whether the YSL regulates Vegfc function. Furthermore, the YSL might be serving as a scaffold for many cell types, including endodermal cells and myocardial cells, which migrate on it. We hypothesize that *mtx1* might be involved in establishing the YSL as a scaffold for cell migration, and therefore loss of *mtx1* function would compromise the motility of many cell types that migrate on the YSL (Fig. 8). This hypothesis is consistent with the fact that *mtx2* in the YSL regulates embryonic cell movements during epiboly (Bruce et al., 2005).

Role of extra-embryonic tissues in vertebrate heart development

Several mutations in mouse, such as those in the fibronectin, *Gata4*, *Mesp1*, *Furin* and *Foxp4* genes, are known to affect the migration of myocardial precursors and lead to cardia bifida (George et al., 1993; Kuo et al., 1997; Molkentin et al., 1997; Roebroek et al., 1998; Saga et al., 1999; Constam and Robertson, 2000; Li et al., 2004). In mouse embryos around embryonic day 7.5, myocardial precursors appear to lie adjacent to the extra-embryonic visceral endoderm (Kaufman, 1992). This scheme might be equivalent to that in zebrafish, in which myocardial precursors migrate on the extra-embryonic YSL. Interestingly, chimeric analyses in mouse have demonstrated that Gata4 function in the visceral endoderm is required for myocardial migration (Watt et al., 2004). Therefore, we speculate that the YSL in zebrafish has a role in myocardial migration equivalent to that of the visceral endoderm in mouse. Several genes, such as *ferroportin1* (Donovan et al., 2000), are expressed in the YSL in zebrafish and the visceral endoderm in mouse, further highlighting the similarities between these two tissues. It will therefore be interesting to assess the role of the visceral endoderm in establishing ECM assembly in mouse embryonic tissues.

We thank Won-Suk Chung for *Tg(sox17:GFP)*^{s870} fish, Le Trinh for sharing unpublished information about *natter* mutants and helpful discussions, Rima Arnaout for critical reading of the manuscript, and the reviewers for constructive feedback. *mtx1* constructs were kindly provided by Drs Tsutomu Hirata and Masahiko Hibi. T.S. was supported by fellowships from the JSPS, the TOYOBO Biotechnology Foundation, and the American Physiological Society, and this work was further supported by grants from the NIH and Packard foundation to D.Y.R.S. T.S. thanks Jun-ichi Sakiyama and Deborah Yelon for helpful discussions.

References

Alexander, J. and Stainier, D. Y. (1999). A molecular pathway leading to endoderm formation in zebrafish. *Curr. Biol.* **9**, 1147-1157.

Alexander, J., Stainier, D. Y. and Yelon, D. (1998). Screening mosaic F1 females for mutations affecting zebrafish heart induction and patterning. *Dev. Genet.* **22**, 288-299.

Alexander, J., Rothenberg, M., Henry, G. L. and Stainier, D. Y. (1999). casanova plays an early and essential role in endoderm formation in zebrafish. *Dev. Biol.* **215**, 343-357.

Beddington, R. S. and Robertson, E. J. (1999). Axis development and early asymmetry in mammals. *Cell* **96**, 195-209.

Brennan, J., Lu, C. C., Norris, D. P., Rodriguez, T. A., Beddington, R. S. and Robertson, E. J. (2001). Nodal signalling in the epiblast patterns the early mouse embryo. *Nature* **411**, 965-969.

Bruce, A. E., Howley, C., Dixon Fox, M. and Ho, R. K. (2005). T-box gene eomesodermin and the homeobox-containing Mix/Bix gene mtx2 regulate epiboly movements in the zebrafish. *Dev. Dyn.* **233**, 105-114.

Chen, J. N., Haffter, P., Odenthal, J., Vogelsang, E., Brand, M., van Eeden, F. J., Furutani-Seiki, M., Granato, M., Hammerschmidt, M., Heisenberg, C. P. et al. (1996). Mutations affecting the cardiovascular system and other internal organs in zebrafish. *Development* **123**, 293-302.

Chen, S. and Kimelman, D. (2000). The role of the yolk syncytial layer in germ layer patterning in zebrafish. *Development* **127**, 4681-4689.

Constam, D. B. and Robertson, E. J. (2000). Tissue-specific requirements for the

proprotein convertase furin/SPC1 during embryonic turning and heart looping. *Development* **127**, 245-254.
Cooper, M. S. and D'Amico, L. A. (1996). A cluster of noninvoluting endocytic cells at the margin of the zebrafish blastoderm marks the site of embryonic shield formation. *Dev. Biol.* **180**, 184-198.
D'Amico, L. A. and Cooper, M. S. (2001). Morphogenetic domains in the yolk syncytial layer of axiating zebrafish embryos. *Dev. Dyn.* **222**, 611-624.
David, N. B. and Rosa, F. M. (2001). Cell autonomous commitment to an endodermal fate and behaviour by activation of Nodal signalling. *Development* **128**, 3937-3947.
de Souza, F. S. and Niehrs, C. (2000). Anterior endoderm and head induction in early vertebrate embryos. *Cell Tissue Res.* **300**, 207-217.
Dickmeis, T., Mourrain, P., Saint-Etienne, L., Fischer, N., Aanstad, P., Clark, M., Strahle, U. and Rosa, F. (2001). A crucial component of the endoderm formation pathway, CASANOVA, is encoded by a novel sox-related gene. *Genes Dev.* **15**, 1487-1492.
Donovan, A., Brownlie, A., Zhou, Y., Shepard, J., Pratt, S. J., Moynihan, J., Paw, B. H., Drejer, A., Barut, B., Zapata, A. et al. (2000). Positional cloning of zebrafish ferroportin1 identifies a conserved vertebrate iron exporter. *Nature* **403**, 776-781.
Field, H. A., Ober, E. A., Roeser, T. and Stainier, D. Y. (2003). Formation of the digestive system in zebrafish. I. Liver morphogenesis. *Dev. Biol.* **253**, 279-290.
George, E. L., Georges-Labouesse, E. N., Patel-King, R. S., Rayburn, H. and Hynes, R. O. (1993). Defects in mesoderm, neural tube and vascular development in mouse embryos lacking fibronectin. *Development* **119**, 1079-1091.
Hart, A. H., Hartley, L., Sourris, K., Stadler, E. S., Li, R., Stanley, E. G., Tam, P. P., Elefanty, A. G. and Robb, L. (2002). Mixl1 is required for axial mesendoderm morphogenesis and patterning in the murine embryo. *Development* **129**, 3597-3608.
Heasman, J. (2002). Morpholino oligos: making sense of antisense? *Dev. Biol.* **243**, 209-214.
Henry, G. L. and Melton, D. A. (1998). Mixer, a homeobox gene required for endoderm development. *Science* **281**, 91-96.
Hirata, T., Yamanaka, Y., Ryu, S. L., Shimizu, T., Yabe, T., Hibi, M. and Hirano, T. (2000). Novel mix-family homeobox genes in zebrafish and their differential regulation. *Biochem. Biophys. Res. Commun.* **271**, 603-609.
Hsu, H. J., Liang, M. R., Chen, C. T. and Chung, B. C. (2006). Pregnenolone stabilizes microtubules and promotes zebrafish embryonic cell movement. *Nature* **439**, 480-483.
Huang, C. J., Tu, C. T., Hsiao, C. D., Hsieh, F. J. and Tsai, H. J. (2003). Germ-line transmission of a myocardium-specific GFP transgene reveals critical regulatory elements in the cardiac myosin light chain 2 promoter of zebrafish. *Dev. Dyn.* **228**, 30-40.
Julich, D., Geisler, R. and Holley, S. A. (2005). Integrinalpha5 and delta/notch signaling have complementary spatiotemporal requirements during zebrafish somitogenesis. *Dev. Cell* **8**, 575-586.
Kaufman, M. H. (1992). *The Atlas of Mouse Development.* London: Elsevier.
Kikuchi, Y., Trinh, L. A., Reiter, J. F., Alexander, J., Yelon, D. and Stainier, D. Y. (2000). The zebrafish bonnie and clyde gene encodes a Mix family homeodomain protein that regulates the generation of endodermal precursors. *Genes Dev.* **14**, 1279-1289.
Kikuchi, Y., Agathon, A., Alexander, J., Thisse, C., Waldron, S., Yelon, D., Thisse, B. and Stainier, D. Y. (2001). casanova encodes a novel Sox-related protein necessary and sufficient for early endoderm formation in zebrafish. *Genes Dev.* **15**, 1493-1505.
Kimmel, C. B. and Law, R. D. (1985). Cell lineage of zebrafish blastomeres. II. Formation of the yolk syncytial layer. *Dev. Biol.* **108**, 86-93.
Kimmel, C. B., Ballard, W. W., Kimmel, S. R., Ullmann, B. and Schilling, T. F. (1995). Stages of embryonic development of the zebrafish. *Dev. Dyn.* **203**, 253-310.
Koshida, S., Kishimoto, Y., Ustumi, H., Shimizu, T., Furutani-Seiki, M., Kondoh, H. and Takada, S. (2005). Integrinalpha5-dependent fibronectin accumulation for maintenance of somite boundaries in zebrafish embryos. *Dev. Cell* **8**, 587-598.
Krauss, S., Johansen, T., Korzh, V. and Fjose, A. (1991). Expression of the zebrafish paired box gene pax[zf-b] during early neurogenesis. *Development* **113**, 1193-1206.
Kuo, C. T., Morrisey, E. E., Anandappa, R., Sigrist, K., Lu, M. M., Parmacek, M. S., Soudais, C. and Leiden, J. M. (1997). GATA4 transcription factor is required for ventral morphogenesis and heart tube formation. *Genes Dev.* **11**, 1048-1060.
Kupperman, E., An, S., Osborne, N., Waldron, S. and Stainier, D. Y. (2000). A sphingosine-1-phosphate receptor regulates cell migration during vertebrate heart development. *Nature* **406**, 192-195.
Leskow, F. C., Holloway, B. A., Wang, H., Mullins, M. C. and Kazanietz, M. G. (2006). The zebrafish homologue of mammalian chimerin Rac-GAPs is implicated in epiboly progression during development. *Proc. Natl. Acad. Sci. USA* **103**, 5373-5378.
Li, S., Zhou, D., Lu, M. M. and Morrisey, E. E. (2004). Advanced cardiac morphogenesis does not require heart tube fusion. *Science* **305**, 1619-1622.
Linask, K. K. and Lash, J. W. (1988). A role for fibronectin in the migration of avian precardiac cells. I. Dose-dependent effects of fibronectin antibody. *Dev. Biol.* **129**, 315-323.
MacFadden, D. G. and Olson, E. N. (2002). Heart development: learning from mistakes. *Curr. Opin. Genet. Dev.* **12**, 328-355.
Mizuno, T., Yamaha, E., Wakahara, M., Kuroiwa, A. and Takeda, H. (1996). Mesoderm induction in zebrafish. *Nature* **383**, 131-132.
Molkentin, J. D., Lin, Q., Duncan, S. A. and Olson, E. N. (1997). Requirement of the transcription factor GATA4 for heart tube formation and ventral morphogenesis. *Genes Dev.* **11**, 1061-1072.
Ober, E. A., Field, H. A. and Stainier, D. Y. (2003). From endoderm formation to liver and pancreas development in zebrafish. *Mech. Dev.* **120**, 5-18.
Ober, E. A., Olofsson, B., Makinen, T., Jin, S. W., Shoji, W., Koh, G. Y., Alitalo, K. and Stainier, D. Y. (2004). Vegfc is required for vascular development and endoderm morphogenesis in zebrafish. *EMBO Rep.* **5**, 78-84.
Oxtoby, E. and Jowett, T. (1993). Cloning of the zebrafish krox-20 gene (krx-20) and its expression during hindbrain development. *Nucleic Acids Res.* **21**, 1087-1095.
Parsons, M. J., Pollard, S. M., Saude, L., Feldman, B., Coutinho, P., Hirst, E. M. and Stemple, D. L. (2002). Zebrafish mutants identify an essential role for laminins in notochord formation. *Development* **129**, 3137-3146.
Pollard, S. M., Parsons, M. J., Kamei, M., Kettleborough, R. N., Thomas, K. A., Pham, V. N., Bae, M. K., Scott, A., Weinstein, B. M. and Stemple, D. L. (2006). Essential and overlapping roles for laminin alpha chains in notochord and blood vessel formation. *Dev. Biol.* **289**, 64-76.
Reiter, J. F., Alexander, J., Rodaway, A., Yelon, D., Patient, R., Holder, N. and Stainier, D. Y. (1999). Gata5 is required for the development of the heart and endoderm in zebrafish. *Genes Dev.* **13**, 2983-2995.
Roebroek, A. J., Umans, L., Pauli, I. G., Robertson, E. J., van Leuven, F., Van de Ven, W. J. and Constam, D. B. (1998). Failure of ventral closure and axial rotation in embryos lacking the proprotein convertase Furin. *Development* **125**, 4863-4876.
Saga, Y., Miyagawa-Tomita, S., Takagi, A., Kitajima, S., Miyazaki, J. and Inoue, T. (1999). MesP1 is expressed in the heart precursor cells and required for the formation of a single heart tube. *Development* **126**, 3437-3447.
Sakaguchi, T., Kuroiwa, A. and Takeda, H. (2001). A novel sox gene, 226D7, acts downstream of Nodal signaling to specify endoderm precursors in zebrafish. *Mech. Dev.* **107**, 25-38.
Sakaguchi, T., Mizuno, T. and Takeda, H. (2002). Formation and patterning roles of the yolk syncytial layer. In *Pattern Formation in Zebrafish* (ed. L. Solnica-Krezel), pp. 1-14. Berlin, Heidelberg, New York: Springer-Verlag.
Stainier, D. Y. (2001). Zebrafish genetics and vertebrate heart formation. *Nat. Rev. Genet.* **2**, 39-48.
Stainier, D. Y., Fouquet, B., Chen, J. N., Warren, K. S., Weinstein, B. M., Meiler, S. E., Mohideen, M. A., Neuhauss, S. C., Solnica-Krezel, L., Schier, A. F. et al. (1996). Mutations affecting the formation and function of the cardiovascular system in the zebrafish embryo. *Development* **123**, 285-292.
Stemple, D. L. (2005). Structure and function of the notochord: an essential organ for chordate development. *Development* **132**, 2503-2512.
Tallafuss, A. and Bally-Cuif, L. (2003). Tracing of her5 progeny in zebrafish transgenics reveals the dynamics of midbrain-hindbrain neurogenesis and maintenance. *Development* **130**, 4307-4323.
Trinh, L. A. and Stainier, D. Y. (2004). Fibronectin regulates epithelial organization during myocardial migration in zebrafish. *Dev. Cell* **6**, 371-382.
Trinkaus, J. P. (1992). The midblastula transition, the YSL transition and the onset of gastrulation in Fundulus. *Dev. Suppl.* 75-80.
Wagner, D. S., Dosch, R., Mintzer, K. A., Wiemelt, A. P. and Mullins, M. C. (2004). Maternal control of development at the midblastula transition and beyond: mutants from the zebrafish II. *Dev. Cell* **6**, 781-790.
Watt, A. J., Battle, M. A., Li, J. and Duncan, S. A. (2004). GATA4 is essential for formation of the proepicardium and regulates cardiogenesis. *Proc. Natl. Acad. Sci. USA* **101**, 12573-12578.
Weinberg, E. S., Allende, M. L., Kelly, C. S., Abdelhamid, A., Murakami, T., Andermann, P., Doerre, O. G., Grunwald, D. J. and Riggleman, B. (1996). Developmental regulation of zebrafish MyoD in wild-type, no tail and spadetail embryos. *Development* **122**, 271-280.
Yelon, D., Horne, S. A. and Stainier, D. Y. (1999). Restricted expression of cardiac myosin genes reveals regulated aspects of heart tube assembly in zebrafish. *Dev. Biol.* **214**, 23-37.